where y_H and y_n represent the activity coefficients of the proton and a protonated species H_nL. Since the relative partial molar enthalpy $\bar{l}_i$ is generally given by

$$-\frac{\bar{l}_i}{RT^2} = \left(\frac{\partial \ln y_i}{\partial T}\right)_{P,n_j} \quad \text{(A3)}$$

partial differentiation of eq A2 with respect to temperature results in

$$\Delta\Delta H_n = \Delta H_n^C - \Delta H_n^T = \bar{l}_n - \bar{l}_{n-1} - \bar{l}_H \quad \text{(A4)}$$

where ΔH_n^C and ΔH_n^T are changes in enthalpy at a given ionic strength and at infinite dilution, respectively. The value of the right-hand side of eq A4 for PhDTA may not differ largely from that for EDTA, because both ligands are similar from an electrostatic point of view. As the complexation of potassium ion is considerably weaker than that of sodium ion,[21] it follows that $\Delta\Delta H_n(I = 1\text{-}0.1\ M)/(kJ/mol) = -26.5 + 23.7 = -2.8$ from the results for EDTA[22] summarized in Table I. Hence, the intrinsic enthalpy change $-\Delta H_{HL}/(kJ/mol)$ can be calculated as 1.9 (=4.7 - 2.8) for PhDTA at $I = 0.1$ M. This value may be compared more straightforwardly with that of EDTA or CyDTA at $I = 0.1$ M (KNO_3).[9] The less exothermic protonation of PhDTA is now clear.

The second protonation is less complicated, because an alkali-metal ion bonds to HL much more weakly. This is reflected in similar $-\Delta H$ values of EDTA for a potassium nitrate (24.10 kJ/mol, I =1 M) and for a sodium perchlorate medium (24.14 kJ/mol, I = 1 M).[22]

Registry No. PhDTA, 40774-59-2.

(21) Watters, J. I.; Schupp, O. E. *J. Inorg. Nucl. Chem.* **1968**, *30*, 3359.
(22) Vasil'ev, V. P.; Lochergina, L. A.; Yastrebova, T. D. *Zh. Obshch. Khim.* (a) **1973**, *43*, 975. (b) *Ibid.* **1974**, *44*, 1371.

Contribution from the Corporate Research Science Laboratories, Exxon Research and Engineering Company, Annandale, New Jersey 08801

Electronic Structures of Cluster Compounds of MoS_4^{2-}, $Mo_3S_9^{2-}$, and $Ni(MoS_4)_2^{2-}$ by XPS Studies

K. S. Liang,* J. Bernholc,† W.-H. Pan,‡ G. J. Hughes, and E. I. Stiefel

Received April 28, 1986

XPS studies were performed on cluster compounds $(TEA)_2MoS_4$, $(TEA)_2Mo_3S_9$, and $(TEA)_2Ni(MoS_4)_2$ (TEA = tetraethylammonium). The results are analyzed on the basis of formal charge and molecular orbital considerations. The major features of the valence band spectra of $(TEA)_2MoS_4$ and $(TEA)_2Mo_3S_9$ are in good agreement with theoretical densities of states of recent calculations using the local density pseudopotential method. However, the XPS data show that the multiple excitation process is quite significant in the simple tetrahedral MoS_4^{2-}. The XPS of $(TEA)_2Ni(MoS_4)_2$ reveals a significant difference from the XPS of the other two compounds in the top valence band, which is attributed to the additional d electrons in Ni (formally d^8) compared to Mo (formally d^2).

Introduction

The ions MoS_4^{2-}, and $Mo_3S_6^{2-}$, and $Ni(MoS_4)_2^{2-}$ belong to a large class of compounds that serve as models of active sites in molybdoenzymes[1] and for many hydrodesulfurization and hydrodenitrogenation catalysts.[2] An ultimate goal is to reach an electronic structural understanding for the nature of these chemical activities.[3-6] To this end, extensive theoretical work has been carried out recently on several Mo–S complexes[3] and transition-metal sulfide materials[4,5] to examine their bonding properties, frontier orbitals and charge distribution. In contrast, relatively little experimental work probing the electronic properties of these phenomena exists.[6,7] Here the results of experimental studies of $(TEA)_2MoS_4$, $(TEA)_2Mo_3S_9$, and $(TEA)_2Ni(MoS_4)_2$ (TEA = tetraethylammonium) are reported. These studies were performed by using X-ray photoelectron spectroscopy (XPS). Where possible, these results are directly compared with theory.

Photoelectron spectroscopy measures the distribution of the photoexcited electrons, which, in many cases, can be directly compared with the ground-state properties such as the valence band density of states (DOS). Theoretical calculations were performed by using the local density pseudopotential method for molecules as previously described.[8] In this method the electrons are represented by effective one-electron wave functions. The "average" exchange and correlation contributions are included via a one-electron exchange-correlation potential. The core electrons are represented by an angular momentum dependent pseudopotential (effective core potential), whereby only valence electrons enter the calculations. The interpretation of the results is thus as simple as in the extended Hückel theory. The method is, however, first-principle and parameter free.

Experimental Section

$(TEA)_2MoS_4$ was prepared by the metathesis reaction of $(NH_4)_2MoS_4$ with (TEA)OH in methanol solution.[9] The MoS_4^{2-} anions have a regular tetrahedral structure.[10] $(TEA)_2Mo_3S_9$ was synthesized by the thermal reaction of MoS_4^{2-} in DMF solution under anaerobic conditions.[11] The anion $Mo_3S_9^{2-}$ formally consists of two MoS_4^{2-} groups each chelating a central MoS_2^+ ion[8] (Figure 1). $(TEA)_2Ni(MoS_4)_2$ was synthesized by the method of Callahan and Piliero.[11] It contains two

† Present address: Department of Physics, North Carolina State University, Raleigh, NC 27695.
‡ Present address: Research Division, W. R. Grace & Co., Columbia, MD 21044.

(1) See, for example: Stiefel, E. I. In *Molybdenum and Molybdenum-Containing Enzymes*; Coughlan, M. P., Ed.; Pergamon: New York, 1980.
(2) See, for example, Stiefel, E. I.; Chianelli, R. R. In *Nitrogen Fixation*; Muller, A., Newton, W. E., Eds.; Plenum: New York, 1983. Halbert, T. R.; Cohen, S. A.; Stiefel, E. I. *Organometallics* **1985**, *4*, 1689.
(3) Bernholc, J.; Stiefel, E. I. *Inorg. Chem.* **1985**, *24*, 1323.
(4) Harris, S.; Chianelli, R. R. *J. Catal.* **1984**, *86*, 400.
(5) Holzwarth, N. A. W.; Harris, S.; Liang, K. S. *Phys. Rev. B: Condens. Matter* **1985**, *32*, 3745.
(6) Liang, K. S.; Hughes, G. J.; Chianelli, R. R. *J. Vac. Sci. Technol. A* **1984**, *2*, 991.
(7) Roxlo, C. B.; Daage, M.; Ruppert, A. F.; Chianelli, R. R. *J. Catal.* **1986**, *100*, 176.
(8) Bernholc, J.; Holzwarth, N. A. W. *J. Chem. Phys.* **1984**, *81*, 3987.
(9) McDonald, J. W.; Friesen, G. D.; Rosenhein, L. D.; Newton, W. E. *Inorg. Chim. Acta* **1983**, *72*, 205.
(10) Kanatzidis, M. G.; Coucouvanis, D. *Acta Crystallogr., Sect. C: Cryst. Struct. Commun. C* **1983**, *39*, 835.
(11) Pan, W.-H.; Leonowicz, M. E.; Stiefel, E. I. *Inorg. Chem.* **1983**, *22*, 672.

0020-1669/87/1326-1422$01.50/0

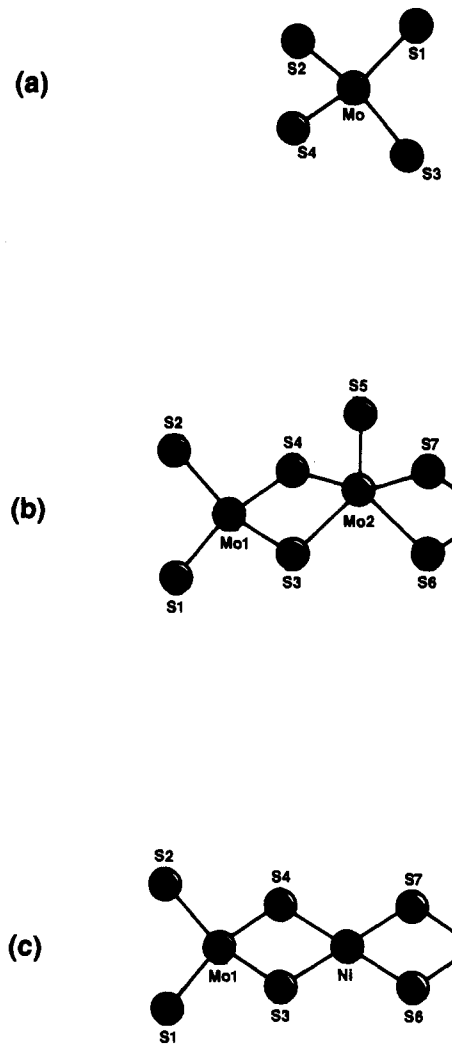

Figure 1. Schematic views of the atomic coordinations of (a) MoS_4^{2-}, (b) $Mo_3S_9^{2-}$ and (c) $Ni(MoS_4)_2^{2-}$ anions.

MoS_4 ligands binding to Ni so as to achieve a square-planar array of S about Ni.[12] Schematic views of the structures of these anions are shown in Figure 1.

XPS measurements were carried out on a Lybold-Heraus LHS-10 spectrometer by following a procedure described previously.[6] The spectrometer is equipped with a dual Mg–Al X-ray source and a hemispherical electron analyzer. Most measurements in this work were performed with the Mg anode ($K\alpha_{1,2}$ photons at 1253.6 eV) operated at 12 KV and 30 mA and the analyzer operated under constant transmission energy (25 eV) mode to achieve good resolution (measured fwhm of Au $4f_{7/2}$ ~0.9 eV). A monochromatized source with the Al anode ($K\alpha_{1,2}$ at 1486.6 eV) was employed only in limited cases to ensure that no speculative contribution from $K\alpha_{3,4}$ photons affected our results.

The measured binding energies for different samples reported in this work are all referred to that of the C 1s level of the TEA cations. The lower binding energy peak of C 1s doublet of TEA is defined to be 285 eV, which is only accurate to within 1 eV on the absolute scale of vacuum level reference. The theoretical curves of the valence bands are shifted in binding energy to match the prominent peak of the experimental ones.

Samples used in this work were first received in the form of small crystals, which were freshly prepared before the study. The crystals were then ground into fine powders inside a glovebox and pressed onto a thin stainless-steel screen used as a support. The samples were then transferred into the spectrometer chamber (base pressure 1.2×10^{-10} Torr). Brief air exposure during the transfer (a few minutes) caused little contamination as judged from the insignificant amount of oxygen observed in the XPS measurements.

The studies were performed at room temperature. Similar to our previous study of $(NH_4)_2MoS_4$,[6] slow surface decomposition of these compounds in vacuum was observed. The decomposition will be discussed in the context of precautions required in the measurements and later as a possible pathway of catalyst formation.

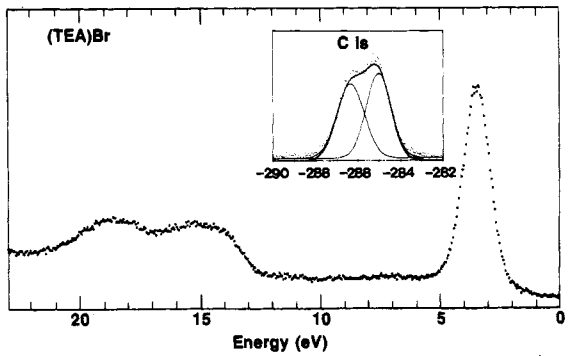

Figure 2. XPS spectra of C 1s and valence band of (TEA)Br.

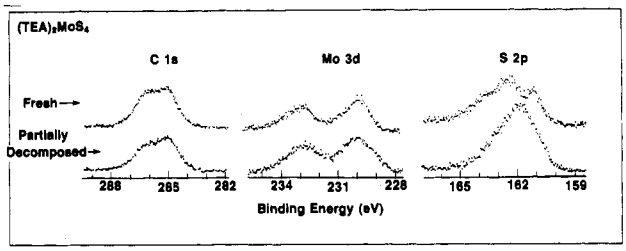

Figure 3. XPS core level spectra of $(TEA)_2MoS_4$ for fresh and partially decomposed states.

Results and Discussion

In this section, the experimental results for each material studied will be discussed, followed by comparison with the theoretical calculation. The experimental data were typically taken in a sequential counting every 15 min for the core level regions and every 30 minutes for the valence band region. The valence band spectra shown in the following are the sum of the two spectra taken in the first hour after the sample was transferred into the vacuum chamber. In this way, we assure that the effect of sample instability is at a minimum. The effect of sample decomposition will be discussed separately at the end of this section.

(TEA)Br. This compound is studied so that the contribution of the $(TEA)^+$ cations in the valence region of other Mo–S compounds can be estimated.

The observed core level spectra of TEA cations can be directly correlated with the bonding of C and N in TEA. The C 1s spectrum can be fitted with two Gausian peaks with equal peak area (Figure 2, inset panel). The peak with higher binding energy (BE) (286.3 eV) is associated with the terminal carbon and the lower binding energy peak (285.0 eV) with the carbon bonded to nitrogen. It is noted that the higher BE peak is broader (fwhm ~ 1.55 eV) than the lower BE one (fwhm ~ 1.38 eV), which is presumably due to a lifetime effect of the photoexcited holes.

The observed valence band of (TEA)Br is shown in Figure 2. The spectrum reveals mainly three peaks at ~3.4, 15, and 18.5 eV. We attribute the first peak (fwhm ~ 1.35 eV) to 4p electrons of Br^- ions and the higher two peaks to hybridized σ bonds of $(TEA)^+$ ions. It is interesting to note the separation of ~12 eV between the valence states of cations and anions. In the Mo–S compounds to be discussed, the two higher energy peaks of TEA will appear along with the valence states of anions.

$(TEA)_2MoS_4$. In $(TEA)_2MoS_4$, one would expect simple core level spectra from Mo and S on the basis of the strict tetrahedral structure of the MoS_4^{2-} anion. Instead, very broad spectra of both Mo 3d and S 2p were observed (Figure 3). The XPS valence band spectrum of $(TEA)_2MoS_4$ reveals similar complication. It shows peaks at ~2.2, 4.5, 6.5, 9.8, 13.2, 15.3, and 19 eV, labeled A, B, X_1, X_2, C, T_1, and T_2, respectively, in Figure 4. We attribute peaks T_1 and T_2 to $(TEA)^+$ ions and peaks A, B, and C to the MoS_4^{2-} ions. Peaks X_1 and X_2 are believed not to be associated with the ground state of this compound.

(12) Callahan, K. P.; Piliero, P. A. *Inorg. Chem.* **1980**, *19*, 2619.
(13) Søtofte, I. *Acta Chem. Scand. Ser. A* **1976**, *A30*, 157.

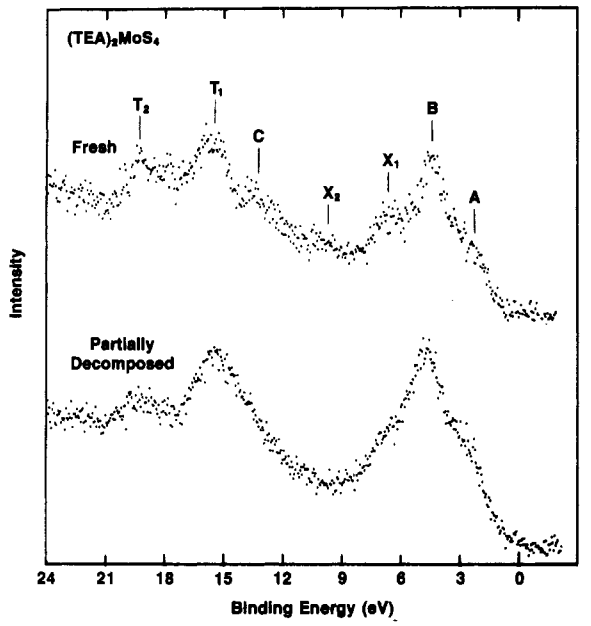

Figure 4. Valence band spectra of $(TEA)_2MoS_4$ for fresh and partially decomposed states.

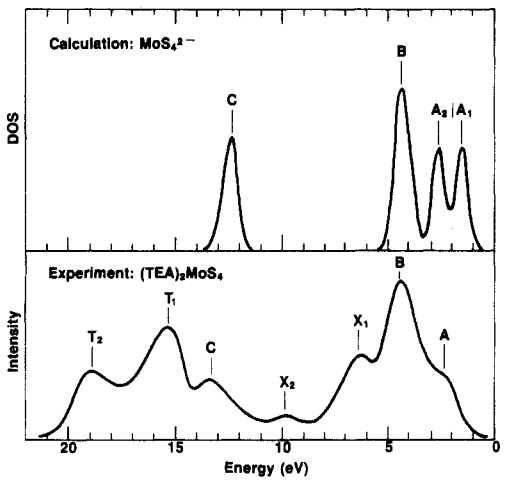

Figure 5. XPS valence spectrum of $(TEA)_2MoS_4$ and theoretical DOS of MoS_4^{2-}. Peaks T_1 and T_2 of the experimental curve are attributed to TEA cations. Peaks X_1 and X_2 are presumably due to multiple excitation in photoemission.

In Figure 5, the experimental spectrum is compared with the theoretical DOS curve. The theoretical DOS is obtained by summation of MO's of a previous calculation[3] using a Gausian width of 0.3 eV for each MO. The experimental curve shown in the figure is obtained after a linear background subtraction and smoothing. The comparison between the calculated DOS and the measured spectrum reveals agreement in the major features but also shows some discrepancy, which is discussed below.

Peak C is primarily associated with the localized bonding states of S 3s and needs no further discussion. We consider mainly the upper valence band under peaks A and B. This band mainly originates from Mo 4d and S 3p electrons. From the calculation, peaks A_1 and A_2 represent one-electron excitations from mainly weakly interacting 3p electrons between S atoms 3.55 Å apart, i.e. the $1t_1$ and $3t_2$ orbitals of tetrahedral MoS_4^{2-} anions. The region under peak B originates from the Mo–S bonding states primarily involving Mo 4d and S 3p electrons.

In Figure 5, we note that the experimental curve shows only a shoulder at the position of peak A_1 of the theoretical DOS. The possible explanations include downshifting due to ion field effect, a small transition probability for the S 3p states, and theoretical uncertainties. Moreover, it is interesting to note that, in our previous UPS study[6] of poorly crystalline MoS_2, band tail states

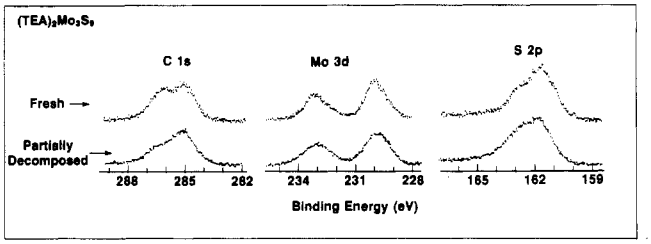

Figure 6. XPS core level spectra of $(TEA)_2Mo_3S_9$ for fresh and partially decomposed states.

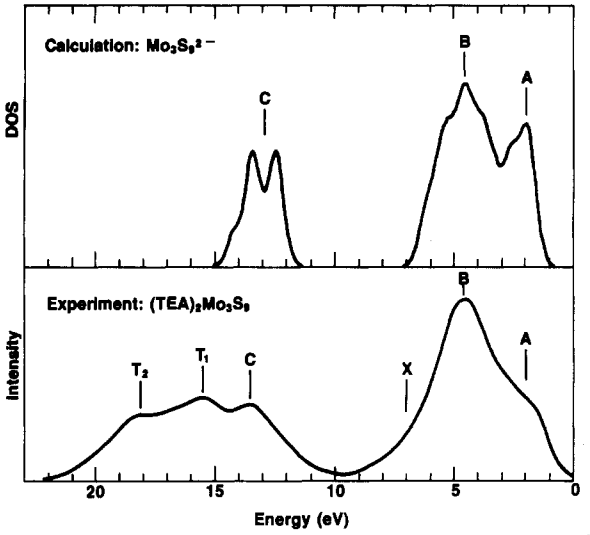

Figure 7. Comparison of experimental and theoretical DOS of $(TEA)_2Mo_3S_9$.

near the top of the valence band were also observed and their presence was shown to be reversible with respect to oxygen adsorption. Although the disappearance of the A_1 peak in the XPS valence band spectrum of $(TEA)_2MoS_4$ might have been related to that observed in MoS_2, the other possible explanations given above indicate that further study is required.

We note that the X_1 peak is located at about 2 eV below peak B. We consider the most probable cause to be multiple excitation in the photoelectric process. Since the HOMO–LUMO gap in MoS_4^{2-} is 2.5 eV, this peak can be explained by a two-electron process involving photoemission of an electron from the Mo–S bonding states simultaneous with a ligand → metal charge-transfer excitation of an additional electron. The X_2 peak was only seen in some of the samples studied, and its origin is not clear to us.

The observed spectrum of the S 2p level of fresh $(TEA)_2MoS_4$ also shows satellite peaks (Figure 3). If we note that a regular S 2p peak has the shape of a spin–orbit split doublet (as seen in Figure 6 for $(TEA)_2Mo_3S_9$), the observed spectrum strongly suggests that a similar multiple excitation of S 2p electrons occurred in $(TEA)_2MoS_4$. A superimposed spectrum of the ground state S 2p and one downshifted by ~2 eV would be consistent with what we observed. We note that the satellite peaks disappear after surface decomposition. We will discuss this later.

$(TEA)_2Mo_3S_9$. Although the XPS spectra of $(TEA)_2MoS_4$ contain complicated features, the results for $(TEA)_2Mo_3S_9$ are relatively straightforward to understand. These results are displayed in Figure 6 for the core levels and in Figure 7 for the valence band. We note that the Mo 3d peak has a normal width of about 1.3 eV in the fresh sample. Attempts to fit the S 2p spectrum with two kinds of sulfur atoms of bridging and terminal types result in a separation of ~1 eV between the resolved peaks.

The background-corrected valence band spectrum of this compound and the theoretical DOS of $Mo_3S_9^{2-}$ are compared in Figure 7. The experimental curve is labeled with five major peaks, A, B, C, T_1, and T_2, at ~2.0, 4.5, 13.0, 15.5 and 18.2 eV, respectively. As in the case of $(TEA)_2MoS_4$, we attribute peaks T_1 and T_2 to $(TEA)^+$ ions and peak C to the bonding states of

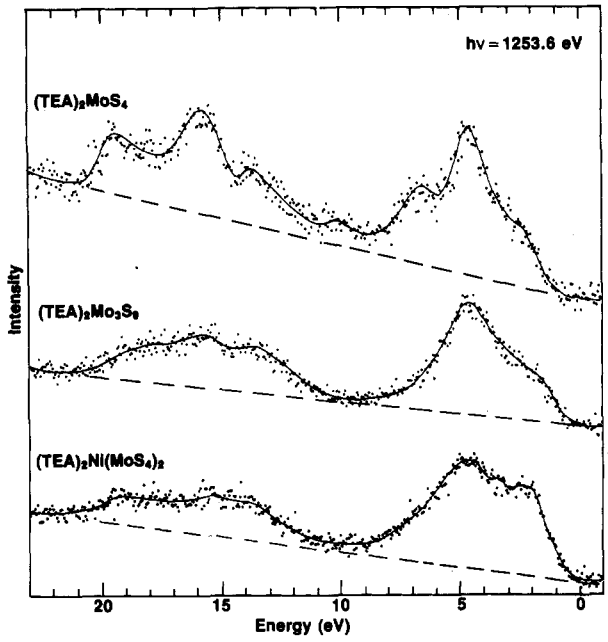

Figure 8. Comparison of DOS of $(TEA)_2NiMo_2S_8$ with those of $(TEA)_2MoS_4$ and $(TEA)_2Mo_3S_9$.

sulfur 3s electrons of MoS_4^{2-} ligands and MoS^{2+} central core ions. The shoulder near 7 eV labeled as X might be associated with two-electron excitation as in $(TEA)_2MoS_4$, although it is much weaker in this case. The weakness could be explained by the delocalization and mixing of orbitals in larger Mo–S clusters, which reduces the probability of multiple excitation. Except for this shoulder region, the observed spectrum agrees overall very well with the theoretical DOS.

One should note that the tops of the valence band (peak A) in $(TEA)_2MoS_4$ and $(TEA)_2Mo_3S_9$ are quite different due to differences in the bonding. The formal electronic configuration of Mo is d^0 in MoS_4^{2-}, but it is d^2 for the central MoS^{2+} unit in $Mo_3S_9^{2-}$. In terms of molecular orbitals, it is shown by the calculations that the two t_1 orbitals from the MoS_4^{2-} ligands mix strongly with the $d_{x^2-y^2}$ orbital of the central MoS^{2+} unit to give contributions to peak A. Therefore, the peak A in $(TEA)_2Mo_3S_9$ contains orbitals with strong d character in addition to the orbitals of mainly S 3p origin as in $(TEA)_2MoS_4$.

$(TEA)_2Ni(MoS_4)_2$. Structurally, $(TEA)_2Ni(MoS_4)_2$ closely resembles $(TEA)_2Mo_3S_9$. The former can be regarded as formed by a formal replacement of the MoS^{2+} central core by Ni^{2+} (Figure 1). We are interested in comparing the electronic structures of these two compounds, in particular the relation to the promotion effect of Ni in Mo–S hydrodesulfurization catalysts.[4]

Figure 8 compares the valence band spectra of the three compounds studied here. It is evident that the intensity at the top band of $(TEA)_2Ni(MoS_4)_2$ is enhanced significantly with respect to the other two. This enhancement is attributed to the fact that there are more d electrons in Ni (formally d^8) than in Mo (formally d^2), leading to observable ligand field splittings at the top of the valence band spectrum. The spectrum of $(TEA)_2Ni(MoS_4)_2$ also indicates the possible presence of a new feature near 3.3 eV. To understand these results in detail, theoretical calculations of this compound are under way. We believe that the understanding of the electronic structure of this compound could shed new light on the promotional effect known in Ni-promoted MoS_2 hydrodesulfurization catalysts.

Pathway of Surface Decomposition. Finally, we comment about our observation that both $(TEA)_2MoS_4$ and $(TEA)_2Mo_3S_9$ are unstable under vacuum (Figures 3, 4, and 6). The changes observed on the core level spectra after ~12 h under vacuum reveal substantial loss of both C and N in the TEA cations (see Figures 3 and 6 for C; N not shown). For the anions, the integrated intensities of the core level peaks of Mo and S remain roughly constant but substantial changes of the peak shapes are evident in S 2p and valence band spectra of $(TEA)_2MoS_4$. This is attributed to the reduction of multiply excited satellite peaks in this compound after decomposition. In our previous XPS study of $(NH_4)_2MoS_4$, similar vacuum instability was also observed.[6]

For $(NH_4)_2MoS_4$, the material is known to be the precursor of an amorphous compound MoS_3 by a thermal decomposition process at ~200 °C.[14] X-ray and XPS studies of MoS_3 revealed that the compound has a unique structure containing both disulfur and singly bonded metal–metal species.[15-17] The disulfur species are easily identified from the XPS S 2p core level and S 3s valence level regions (see Figures 3 and 4 of ref 15). The comparison of the XPS spectra of partially vacuum-decomposed $(TEA)_2MoS_4$ and $(TEA)_2Mo_3S_9$ with that of MoS_3 in these energy regions indicates the presence of disulfur species on the decomposed surfaces. This suggests that in decomposition, MoS_3 could be formed through the cross-linking of the anion clusters. The structural cross-linking would also result in the loss of multiple excitation as observed.

The results of this study suggest that the decomposition of these Mo–S cluster compounds under vacuum goes toward MoS_3 in a pathway similar to thermal decomposition of $(NH_4)_2MoS_4$, although the decomposition in vacuum at room temperature is seen to stop once a new surface layer is formed. These observations might suggest that the instability of the surfaces of these compounds under vacuum is associated with TEA or NH_4 cations because of the observed loss of C and N. However, $(TEA)_2Ni(MoS_4)_2$ showed no sign of decomposition under the same experimental conditions (16 h in vacuum). If the explanation involving cross-linking of Mo–S anions is correct, the heterometallic cluster $Ni(MoS_4)_2^{2-}$ would not have this pathway available to it and consequently could not similarly decompose.

Summary

We have performed XPS studies on three Mo–S cluster compounds, namely $(TEA)_2MoS_4$, $(TEA)_2Mo_3S_9$, and $(TEA)_2Ni(MoS_4)_2$. The results are qualitatively understood on the basis of formal charge and molecular orbital considerations. In the first two compounds, the XPS valence band spectra are also directly compared with theoretical density of states from recent calculations using the local-density pseudopotential method. The agreement in the major features of ground-state electronic structure is in general quite good. The XPS results also suggest that a multiple excitation process may be quite significant in the simple tetrahedral MoS_4^{2-}.

In a manner similar to our previous study of $(NH_4)_2MoS_4$, the surfaces of both $(TEA)_2MoS_4$ and $(TEA)_2Mo_3S_9$ were found to undergo decomposition in vacuum. Our preliminary results indicate that the pathway of the decomposition is similar to that of the thermal decomposition of $(NH_4)_2MoS_4$, which leads to the formation of a unique compound, amorphous MoS_3.

It is interesting to note that $(TEA)_2Ni(MoS_4)_2$, in contrast to the other two compounds, is quite stable under vacuum at room temperature, most likely because the above decomposition route is not available to it. The XPS results of $(TEA)_2Ni(MoS_4)_2$ also show that the d electrons of Ni are located near the top of the occupied valence states. Whether these effects have any significant implication in the understanding of binary Ni–Mo sulfide catalysts is a subject for future research. We are currently extending this study to the related compounds $(TEA)_3Fe(MoS_4)_2$ and $(TEA)_3Co(MoS_4)_2$.

Acknowledgment. We thank T. R. Halbert and R. R. Chianelli for useful discussions. We are also grateful to L. L. Hutchings and S. D. Cameron for help in the experiment.

(14) Jacobson, A. J.; Chianelli, R. R.; Rich, S. M.; Whittingham, M. S. *Mater. Res. Bull.* **1979**, *14*, 1437.
(15) Liang, K. S.; DeNeufville, J. P.; Jacobson, A. J.; Chianelli, R. R.; Betts, F. *J. Non-Cryst. Solids* **1980**, *35 & 36*, 1249.
(16) Cramer, S. P.; Liang, K. S.; Jacobson, A. J.; Chang, C. H.; Chianelli, R. R. *Inorg. Chem.* **1984**, *23*, 1215.
(17) Chien, F. Z.; Moss, S. C.; Liang, K. S.; Chianelli, R. R. *Phys. Rev. B: Condens. Matter* **1984**, *29*, 4606.